Boundary-Layer Meteorology (2019) 170:507–518
https://doi.org/10.1007/s10546-018-0406-y

NOTES AND COMMENTS

Sensitivity of Turbine-Height Wind Speeds to Parameters in the Planetary Boundary-Layer Parametrization Used in the Weather Research and Forecasting Model: Extension to Wintertime Conditions

Larry K. Berg[1] · Ying Liu[1] · Ben Yang[2] · Yun Qian[1] · Joseph Olson[3] · Mikhail Pekour[1] · Po-Lun Ma[1] · Zhangshuan Hou[1]

Received: 21 February 2018 / Accepted: 30 October 2018 / Published online: 16 November 2018

Abstract
We extend the model sensitivity analysis of Yang et al. (Boundary-Layer Meteorol 162: 117–142, 2017) to include results for February 2011, in addition to May of the same year. We investigate the sensitivity of simulated hub-height wind speeds to the selection of 12 parameters applied in the Mellor–Yamada–Nakanishi–Niino planetary boundary-layer parametrization in the Weather Research and Forecasting model, including parameters used to represent the dissipation of turbulence kinetic energy (TKE), Prandtl number (Pr), and turbulence length scales. Differences in the sensitivity of the ensemble of simulated wind speed to the various parameters can largely be explained by changes in the static stability. The largest monthly differences are found during the day, while the sensitivity to many of the parameters during the night is similar regardless of the month. This finding is consistent with an increased frequency of daytime stable conditions in February compared to May. The spatial variability of the sensitivity to TKE dissipation and Pr can also be attributed to variability in the static stability across the domain at any point in time.

Keywords Parametrization schemes · Parametric sensitivity · Planetary boundary layer · Turbine-height wind speed · Weather research and forecasting model

1 Introduction

Yang et al. (2017) explored the sensitivity of simulations completed using the Weather Research and Forecasting (WRF) model for a region in the Pacific North-west of the United

✉ Larry K. Berg
Larry.berg@pnnl.gov

1 Pacific Northwest National Laboratory, P.O. Box 999, Richland, WA 99352, USA

2 CMA-NJU Joint Laboratory for Climate Prediction Studies, Institute for Climate and Global Change Research, School of Atmospheric Sciences, Nanjing University, Nanjing, China

3 University of Colorado/CIRES, Boulder, CO, USA

States for conditions found in the Department of Energy Columbia Basin Wind Energy Study (CBWES; Berg et al. 2012). The primary results of that study indicate that 60% of the variance associated with the perturbed parameter ensemble can be attributed to four parameters applied in the planetary boundary layer (PBL) parametrization: the turbulence kinetic energy (TKE) dissipation rate, the turbulent Prandtl number (Pr), and turbulent length scales in the Mellor–Yamada–Nakanishi–Niino (MYNN; Nakanishi 2001; Nakanishi and Niino 2004, 2009) PBL scheme.

The analysis of Yang et al. (2017) focused on May 2011 since there is typically a large wind-energy resource over the Columbia River Basin during May. Other months, however, also have extensive periods of strong winds, and there could be differences in the behaviour of the PBL parametrization when a range of different conditions are considered. For example, there are systematic differences in the occurrence of positive and negative values of the sensible heat flux and values of TKE across different seasons. As an example, Fig. 1 shows the time series of sensible heat flux and TKE measured at 3 m above the ground from 19 January 2011 through 18 April 2011 at the CBWES site. For this reason, a second set of simulations have been completed for February 2011 to evaluate the model sensitivity over a wider range of conditions, and an analysis identical to that of Yang et al. (2017) has been carried out using the same model configuration and sensitivity analysis framework. The goal of the present note is to describe key differences in the parametric sensitivity between the February and May ensembles. While not covering all seasons, these results provide additional insight into the model sensitivities for other months of the year.

2 Methodology

The model configuration and methodology applied herein are the same as those used and described in Yang et al. (2017), and they are only briefly revisited here. In all, 256 additional simulations were carried out for February 2011 using the WRF model (Skamarock et al. 2008), and with two different computational domains, an outer grid with 10-km horizontal grid spacing and an inner grid with 3.3-km grid spacing. Initial and boundary conditions for

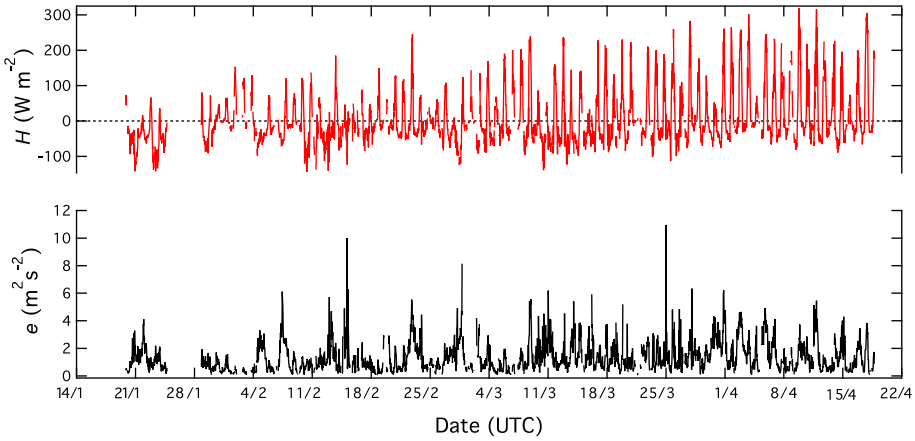

Fig. 1 Time series of sensible heat flux, H (top) and TKE, e (bottom) measured using a sonic anemometer mounted 3 m above ground at the CBWES field site between 19 January (19/1) and 18 April (18/4) 2011 when the sonic anemometer was relocated to the tall tower at the CBWES site

the simulations were derived from the North American Regional Reanalysis (Mesinger et al. 2006). The last step of the analysis process is to use the WRF model ensemble as input to a generalized linear model that is used to evaluate the sensitivity of the simulated wind speed to the parameter values.

As in the initial study, we focus on 12 parameters within the MYNN PBL scheme. A total of 256 parameter sets was generated using a quasi-Monte Carlo method and applied in the WRF-model simulations as described above. The range of parameter values was determined based on values that have appeared in the literature or, in cases in which such guidance is not available, individual parameter values were changed by $\pm 50\%$.

3 February Results

Following Yang et al. (2017), results from the February and May ensembles are presented in terms of the mean wind speed at 80 m above the ground, spatial distributions of the parametric uncertainty over the model domain as well as at select locations, and simulated vertical wind-speed profiles at the CBWES site. In their study, Yang et al. (2017) defined daytime as between 0600 and 1800 local time (LT) and nighttime between 1800 and 0600 LT. In February, the days are shorter, and tests were completed using day/night thresholds of 0700–1600 LT and 1700–0600 LT for daytime and nighttime conditions, respectively. The results are nearly the same using either definition (not shown), so we apply the definition used by Yang et al. (2017) to ease comparison with their study.

The mean daytime (0600–1800 LT) simulated wind speed at 80 m above the surface is larger for the ensemble of 256 PBL simulations completed for February 2011 than for the May 2011 ensemble (Fig. 2). The differences in simulated ensemble-mean wind speed are generally smaller at night (1800–0600 LT) than during the daytime. The pattern of the ensemble variance is generally independent of the month, and larger values of variance are found at night. Yang et al. (2017) also presented results showing the sensitivity to parameters used in the surface-layer parametrization, but the variance associated with those parameters is independent of the month and does not change significantly between daytime and nighttime (not shown). For this reason, the subsequent discussion only focuses on parameters associated with the PBL parametrization.

3.1 Spatial Distribution of Parametric Sensitivity

One of the primary findings in Yang et al. (2017) is that more than 60% of the total variance in the simulation ensemble is associated with the TKE dissipation rate (B_1), turbulent Prandtl number (Pr), and a subset of constants associated with the turbulent length scales applied in the MYNN PBL scheme (β and α_5). Analysis of the February ensemble confirms that the same subset of parameters is also important at night, but there are notable differences in the daytime results for February and May (Fig. 3). The value of B_1 makes the largest contribution to the ensemble variance during the daytime and is more than 40% of the total variance at many locations in May, but accounts for 60% or more of the variance in February, particularly over areas of elevated terrain. The daytime values of variance associated with Pr variations in the February ensemble are also larger than those found for May, with peak wintertime values accounting for more than 40% of the variance over the basin and smaller contributions over higher terrain. The daytime sensitivity to the value of α_5 is larger in February over the basin and contributes up to 20% of the variance, but it is generally smaller over higher terrain. In

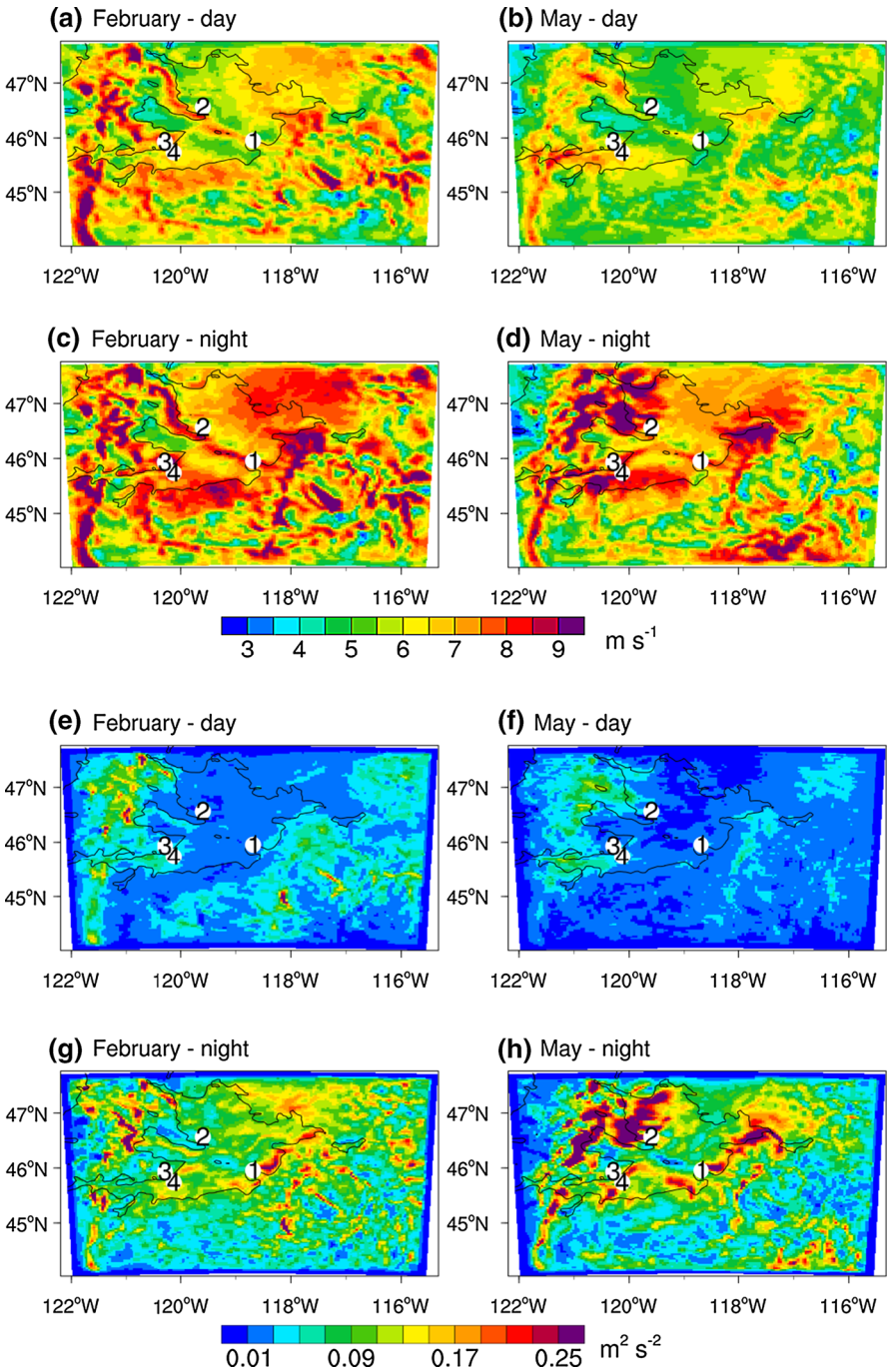

Fig. 2 Spatial distributions of mean wind speed computed from all 256 simulations during February (**a** and **c**) and May (**b** and **d**), and the variance in the ensemble of PBL simulations during February (**e** and **g**) and May (**f** and **h**) for daytime (**a**, **b**, **e** and **f**) and nighttime (**c**, **d**, **g**, and **h**). Numbers indicate the CBWES site (1), Hanford (2), Big Horn (3), and Pebble Springs (4)

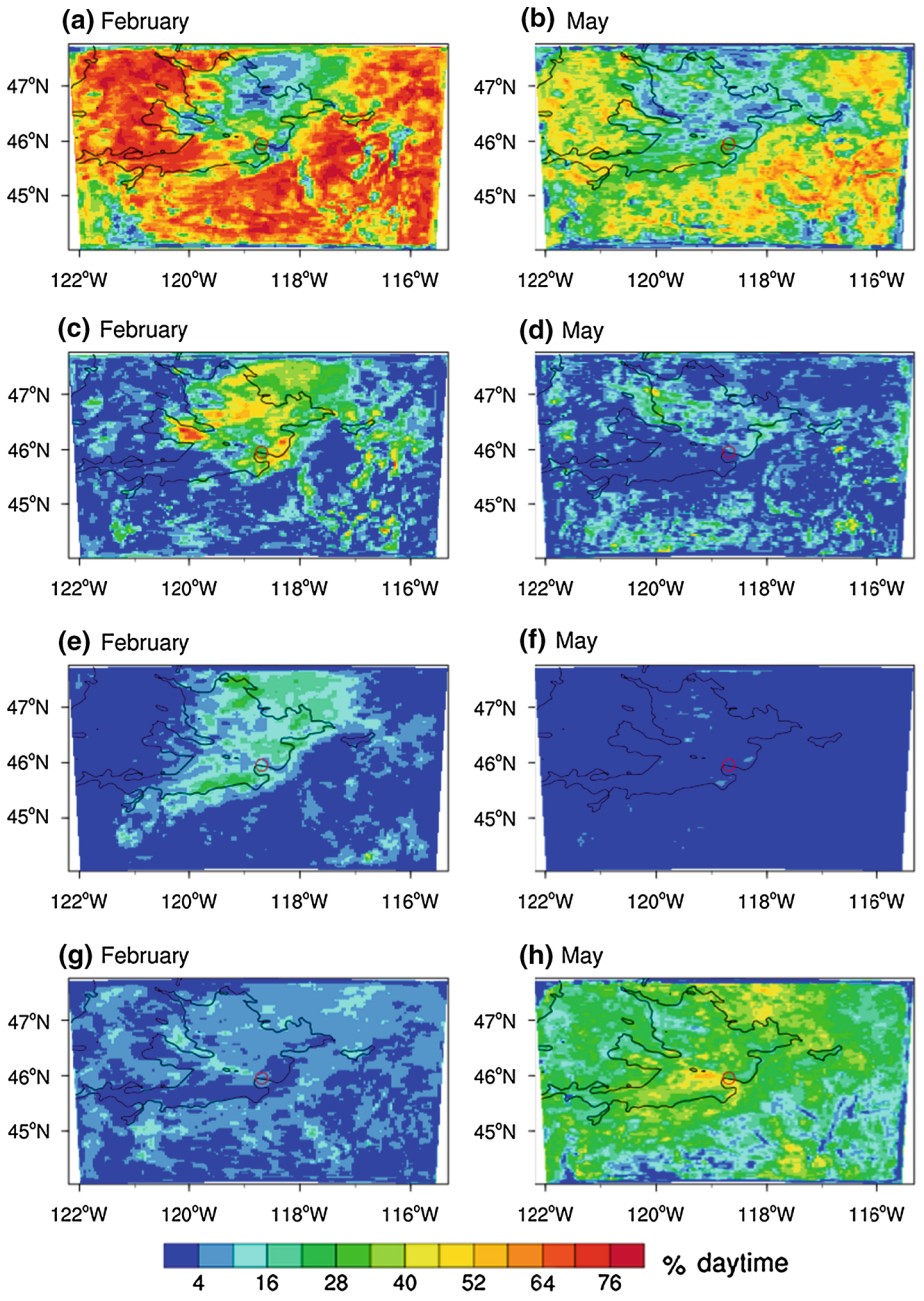

Fig. 3 Spatial distributions of relative contributions (in %) of key parameters to the generalized-linear-model estimated total variances of the 80-m daytime wind speed during February (left column) and May (right column) for B_1 (**a** and **b**), Pr (**c** and **d**), α_5 (**e** and **f**), and β (**g** and **h**). The location of the CBWES site is marked by the red circle in each plot, and the contour represents an elevation of 500 m and the approximate location of the Columbia Basin

contrast, during the daytime in May the contribution to the variance associated with α_5 is negligible. The large daytime differences in the various parameters are likely due to a greater frequency of stable conditions during the daytime in February compared to May.

The nighttime differences (Fig. 4) between the February and May ensembles are generally much smaller than those found in daytime. While there are monthly differences in the magnitudes of the variance associated with each parameter, the same parameters accounts for most of the variance regardless of the month. The relative similarity between the nighttime ensembles is likely due to a similar frequency of stable conditions regardless of the month.

3.2 Parametric Sensitivity at Select Locations

Yang et al. (2017) evaluated the response of the ensembles at four different locations: the CBWES site, Hanford, Big Horn, and Pebble Springs for the four most influential parameters. Big Horn and Pebble Springs sites were selected because they represent wind farms in the Columbia Basin, while Hanford is a Department of Energy (DOE) facility and has a long record of measurements made from a tall tower. In the present analysis, the deviation from the ensemble mean is represented for daytime conditions in both February and May (Fig. 5). Similar to the results shown in Figs. 3 and 4, there are monthly differences in the response to α_5, with the deviation of wind speed increasing when the value of α_5 increases in February (there was very little sensitivity to the value of α_5 during daytime conditions in May). Interestingly, there are also monthly differences in the response to Pr variations at the CBWES and Hanford sites, in which increasing values of Pr lead to a reduction in the daytime wind speeds in February. In contrast, the sensitivity is smaller at the Big Horn and Pebble Springs sites with very little difference in results for February and May. This result could be associated with the location of the sites, as shown in Figs. 3 and 4, where the monthly differences during the day are larger over the basin than in other locations within the domain. As described in the previous section, the nighttime differences are small and are excluded here for brevity.

3.3 Vertical Wind-Speed Profiles

Observations from the CBWES site highlight the frequent occurrence of low-level jets at the site (Yang et al. 2013) in May, and the simulations conducted by Yang et al. (2017) bear this out. During February, however, the low-level jet is less pronounced in both the observations and the ensemble of simulations. On average, there is still a diurnal cycle in the sensitivity to B_1, Pr, and α_5 with the largest spread associated with these variables occurring at night regardless of the month (Fig. 6). There are, however, still significant monthly differences. During May, the results are sensitive to the variation of B_1 to altitudes as high as 900 m above the surface with wind speeds decreasing as the value of B_1 increases. An opposite trend is seen at night, where the wind speed increases as the value of B_1 increases for altitudes above 100 m. The daytime response to changes in B_1 is muted for the February simulations, although the impact remains large at night. The simulations are more sensitive to the value of Pr at night, regardless of the month, although the magnitude of the sensitivity is slightly larger in February than May. The value of α_5 is only applied in statically stable conditions and thus has a larger impact at night than during the day and is limited to approximately the lowest 300 m. As with Pr, α_5 has a larger impact in the winter than the summer, which could be attributed to either greater stability conditions, or more frequent stable conditions

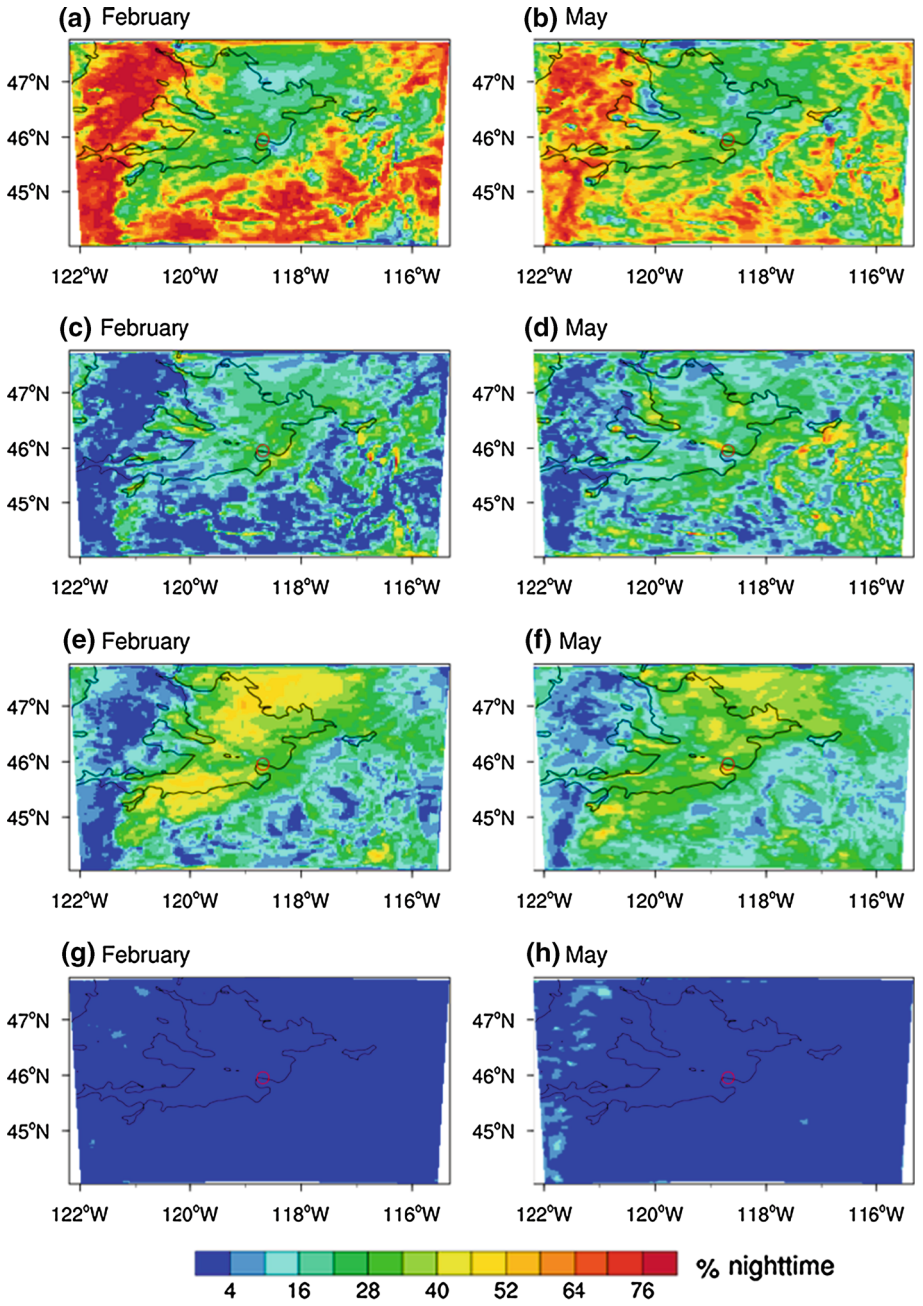

Fig. 4 Spatial distributions of relative contributions (in %) of key parameters to the generalized-linear-model estimated total variances of the 80-m nighttime wind speed during February (left column) and May (right column) for B_1 (**a** and **b**), Pr (**c** and **d**), α_5 (**e** and **f**), and β (**g** and **h**). The location of the CBWES site is marked by the red circle in each plot, and the contour represents an elevation of 500 m and the approximate location of the Columbia Basin

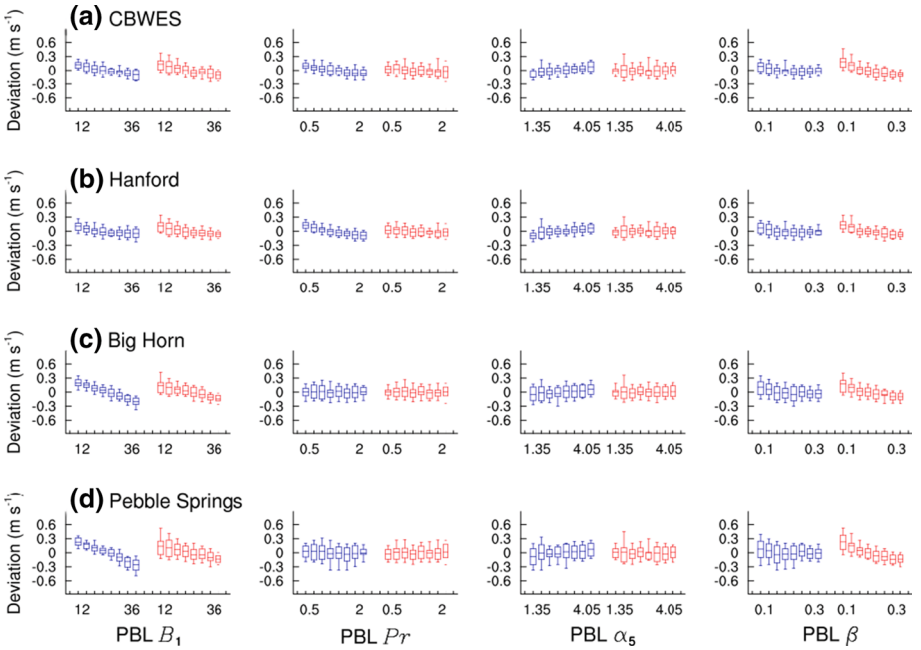

Fig. 5 Averaged daytime sensitivities in February (blue) and May (red) 80-m wind speeds at **a** CBWES, **b** Hanford, **c** Big Horn, and **d** Pebble Springs sites, in response to the perturbations of the four most influential parameters (indicated at the bottom of each column) from the 256 simulations in the ensemble. The 256 simulations are divided into eight discreet bins (each bin with 32 experiments) in terms of each parameter value. In each bin, the mean, 25 to 75th percentile, and 10 to 90th percentile values are presented as box-and-whisker plots. Note that the values are deviations from the overall ensemble mean

during the winter. The response of β, and k, is strongest during the day and show very little dependence on the season (not shown).

4 Discussion

The differences in the sensitivity to the four parameters is largely explained by the static stability and its distribution across the domain. An increased frequency of daytime stable conditions occurs during February compared to May due to lower sun angle, shorter days, as well as higher albedo associated with snow or fog within valley cold pools. Example cumulative distributions of surface sensible heat fluxes, taken from the first ensemble member for the four sites, are shown in Fig. 7. There is generally very little difference in the cumulative distributions of the night-time surface fluxes, and much larger differences during the day. Similar results were seen for different ensemble members (not shown).

The approach used to calculate the length scales in the MYNN parametrization changes with stability, so differences in the sensitivity are expected with the variation of stability. The parameter α_5 is only used in the calculation of length scales in stable conditions. Thus, one would expect an increase in the sensitivity to α_5 with the increase in frequency of stable conditions. The sensitivity to β is opposite to that of α_5 as it is only applied in length scale

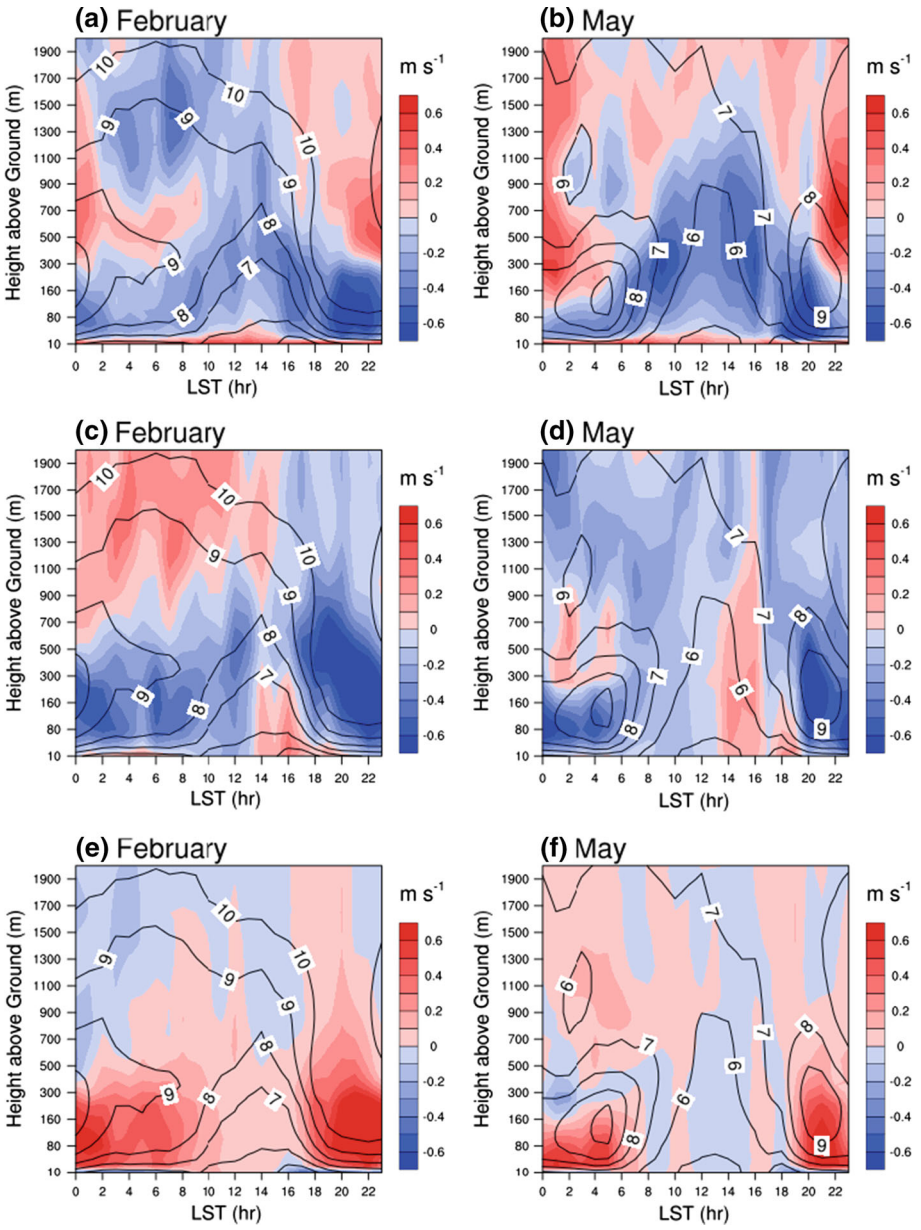

Fig. 6 Vertical distributions of diurnal responses defined as the difference in response for the first and last bin of the sorted data (bin8-bin1 differences) of wind speed (m s^{-1}) at the CBWES field site to the three most influential parameters with significant seasonal differences in the PBL scheme for B_1 (**a** and **b**), Pr (**c** and **d**), and α_5 (**e** and **f**). The simulation ensemble means of wind speed are indicated by the black contours. Red (blue) implies an increase (decrease) in wind speeds with corresponding increase in the value of the parameter tested

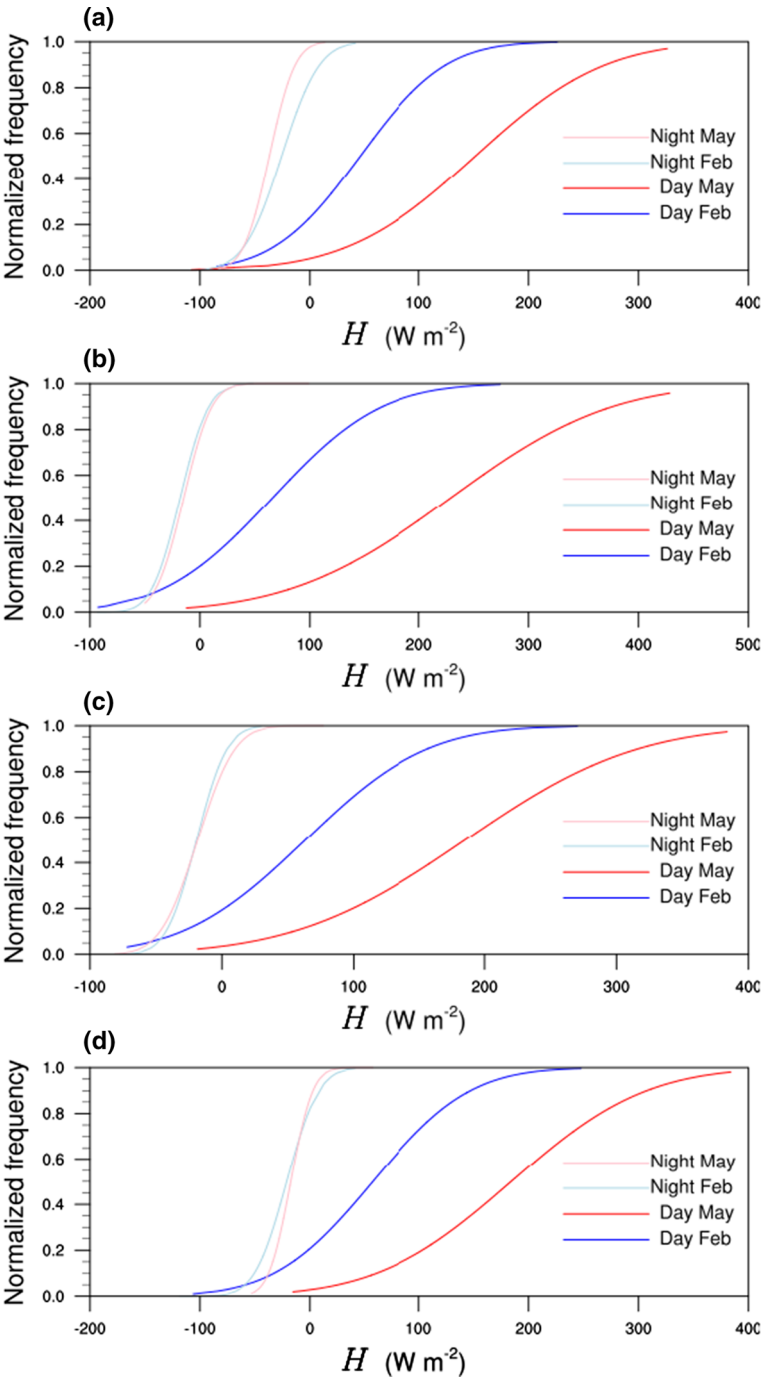

Fig. 7 Cumulative distributions of simulated sensible heat flux (H) at the CBWES, Hanford, Big Horn, and Pebble Springs sites in February (blue) and May (red) during both night (light) and day (dark) for the first ensemble member at the **a** CBWES, **b** Hanford, **c** Big Horn, and **b** Pebble Springs sites

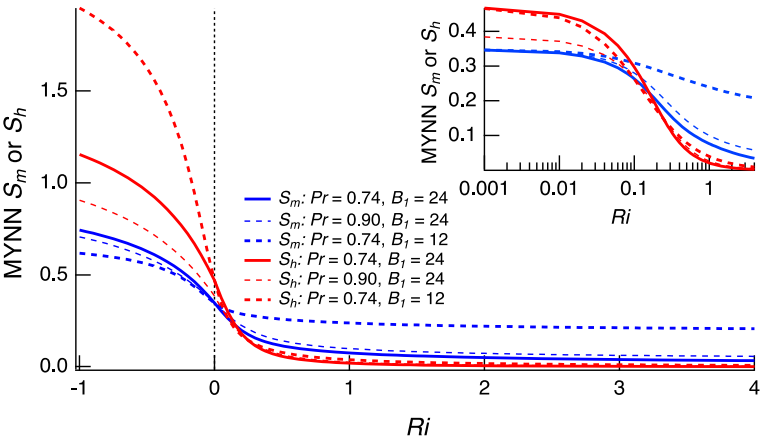

Fig. 8 Variation of MYNN exchange coefficients for momentum (S_m: blue) and heat (S_h: red) for different values of B_1 and Pr as a function of Ri. Inset shows behaviour for values of Ri ranging from 0.001 to 1

calculations in unstable conditions. Therefore, the greatest sensitivity to β is found during daytime conditions in May.

The increased sensitivity of the simulations to Pr variations found over the basin during the daytime in February is more surprising. In the formulation of all Mellor–Yamada-type PBL parametrizations, the values of B_1 and Pr affect the exchange coefficients used for heat and momentum regardless of the stability (noting that B_1 also affects the TKE through the dissipation rate). We see (in Figs. 3 and 4) that the sensitivities to Pr and B_1 are dependent on location, and points with a large sensitivity to Pr tend to have a small sensitivity to B_1. This behaviour is explained, at least in part, by differences in the exchange coefficients as a function of stability. These coefficients have a larger sensitivity to B_1 when the Richardson number (Ri) is relatively large or small (including negative values) as shown by the differences in the broken lines for S_m and S_h in Fig. 8. Points in the domain with large sensitivity to Pr have values of Ri between 0 and 1 during the periods of interest (not shown), and are more commonly found to have lower elevations. As shown in the inset panel of Fig. 8, over these values of Ri, the values of S_m and S_h are more sensitive to changes in Pr than B_1.

5 Summary

We have focused on February and May cases as we expect them to bound the sensitivities at the various sites during both warm and cold seasons in the Columbia Basin. Consistent with the results in Yang et al. (2017), the ensemble of simulations was found to be sensitive to B_1, Pr, and the length scales (α_5 and β). There was little overall difference in the sensitivities found for the February and May ensembles at night. In contrast, there was a significant change in the contributions of Pr, α_5 and β during the day, with greater sensitivity to Pr and α_5 in February and β in May.

While conditions through the summer are probably warmer than those found in May we do not expect there to be large differences in the frequency of stable versus unstable conditions—which likely explains the differences found for the February and May ensembles.

Likewise, similar differences would be expected if we were to consider conditions in autumn that would be associated with a different frequency of stable and unstable conditions.

Acknowledgements This work has been supported by the U.S. Department of Energy's Wind Power Program. The Pacific Northwest National Laboratory (PNNL) is operated for the US Department of Energy by Battelle Memorial Institute under contract DE-AC07-76RL01830. The PNNL Institutional Computing (PIC) provided computational resources. The NARR datasets were freely obtained from the CISL Research Data Archive at http://rda.ucar.edu/datasets/ds608.0/. WRF model output data used in this study are stored at PNNL and are available upon request from the corresponding author. Data from CBWES are available from the U.S. Department of Energy Atmospheric Radiation Measurement (ARM) data archive. Dr. Ben Kravitz (PNNL) is thanked for his comments on an earlier version of the manuscript.

References

Berg LK, Pekour M, Nelson D (2012) Description of the Columbia Basin wind energy study (CBWES). PNNL-22036. Pacific Northwest National Laboratory

Mesinger F, DiMego G, Kalnay E, Mitchell K, Shafran PC, Ebisuzaki W, Jović D, Woollen J, Rogers E, Berbery EH, Ek MB, Fan Y, Grumbine R, Higgins W, Li H, Lin Y, Manikin G, Parrish D, Shi W (2006) North American regional reanalysis. Bull Am Meteorol Soc 87(3):343–360

Nakanishi M (2001) Improvement of the Mellor-Yamada turbulence closure model based on large-eddy simulation data. Boundary-Layer Meteorol 99(3):349–378

Nakanishi M, Niino H (2004) An improved Mellor-Yamada level-3 model with condensation physics: its design and verification. Boundary-Layer Meteorol 112(1):1–31

Nakanishi M, Niino H (2009) Development of an improved turbulence closure model for the atmospheric boundary layer. J Meteorol Soc Jpn 87(5):895–912

Skamarock WC, Klemp JB, Dudhia J, Gill DO, Barker DM, Duda MG, Huang X-Y, Wang W, Powers JG (2008) A description of the advanced research WRF version 3. NCAR/TN-475 + STR. NCAR

Yang Q, Berg LK, Pekour M, Fast JD, Newsom RK, Stoelinga M, Finley C (2013) Evaluation of WRF-predicted near-hub-height winds and ramp events over a Pacific Northwest site with complex terrain. J Appl Meteorol Climatol 52:1753–1763

Yang B, Qian Y, Berg LK, Ma P-L, Wharton S, Bulaevskaya V, Yan H, Hou Z, Shaw WJ (2017) Sensitivity of turbine-height wind speeds to parameters in planetary boundary-layer and surface-layer schemes in the Weather Research and Forecasting model. Boundary-Layer Meteorol 162(1):117–142